CHEMICAL ENGINEERING TRANSACTIONS
VOL. 84, 2021
A publication of AIDIC
The Italian Association of Chemical Engineering
Online at www.cetjournal.it
Guest Editors: Paolo Ciambelli, Luca Di Palma

ISBN 978-88-95608-82-2; **ISSN** 2283-9216

Chemogenic *versus* Biogenic Synthesis of Selenium Nanoparticles: A Structural Characterization

Elena Piacenza[a,*], Alessandro Presentato[a], Francesco Ferrante[b], Delia F. Chillura Martino[a]

[a]Dipartimento di Scienze e Tecnologie Biologiche, Chimiche e Farmaceutiche (STEBICEF), Università degli Studi di Palermo, Viale delle Scienze Ed. 16, 90128, Palermo, Italy
[b]Dipartimento di Fisica e Chimica (DIFC) Emilio Segrè, Università degli Studi di Palermo, Viale delle Scienze Ed. 17, 90128, Palermo, Italy
Corresponding author: elena.piacenza91@gmail.com

Among the plethora of available metal- and metalloid-based nanomaterials (NMs), selenium nanostructures (SeNSs) are one of the most interesting from an applicative perspective due to their intermediate properties between metals and non-metals, as well as their high biocompatibility. In this regard, the capability of microorganisms to biotransform toxic Se-oxyanions – *i.e.*, selenite (SeO_3^{2-}) and selenate (SeO_4^{2-}) – into their less bioavailable elemental forms [Se(0)], mostly generating Se nanoparticles (SeNPs), represents as a useful and *green* alternative over chemogenic synthesis allowing to obtain highly thermodynamically stable NMs. However, their structural characterization, in terms of biomolecules and interactions stabilizing the biogenic colloidal solution, is still a black hole in the microbial nanotechnology field, impairing the exploitation of biogenic SeNP full potential.
Here, a parallel characterization between biogenic and chemogenic SeNPs was carried out through Fourier Transform Infrared spectroscopy in Attenuated Total Reflectance (ATR-FTIR) mode, Nuclear Magnetic Resonance (NMR) spectroscopy, and Density Functional Theory (DFT) calculations, to better understand which functional groups, hence biomolecules, contribute the most to the stabilization of biogenic SeNPs.

1. Introduction

The rapid and exponential growth of nanotechnology during the last 40 years has led to the development of many synthetic procedures to generate nanomaterials (NMs) featuring different sizes, shapes, and compositions for various (bio)technological purposes (Rao et al., 2004). Particularly, SeNSs have gained technological interest due to their physical-chemical versatility (Piacenza et al., 2018a) and their biocompatibility, being Se an essential micronutrient for living organisms, enabling SeNSs biotechnological and biomedical applications (Khurana et al., 2019). Although chemogenic procedures lead to high-quality SeNSs, these approaches mostly rely on dangerous operational conditions and toxic reagents (Piacenza et al., 2018a), forcing to find alternative synthetic methodologies to produce *green* SeNMs, as those based on environmental-friendly and biocompatible chemical reagents or microorganisms (Shoeibi et al., 2017). As opposed to conventional chemogenic syntheses, biogenic approaches give spontaneously rise to thermodynamically stable yet structurally diverse SeNS products, avoiding the need for post-production treatments before their use (Piacenza et al., 2018b). However, the problem that prevents the translation of either chemogenic or biogenic SeNMs from benchtop research to their practical application is a lack of understanding of their structure-to-property relationships as compared to other nanotechnological products.
In the present study, new insights on the structure of SeNSs, and their behavior with respect to the physical and chemical proximities, were put forward by performing ATR-FTIR and ^{1}H-NMR spectroscopies on (i) SeNPs synthesized through a chemogenic yet eco-sustainable procedure involving L-cysteine (Li et al., 2010), and (ii) those produced by the environmental isolate *Micromonospora chokoriensis* grown in the presence of sodium selenite (Na_2SeO_3). Moreover, given the complexity of the systems here analysed, DFT calculations

on SeNP models were carried out to confirm the results obtained from the experimental measurements, gaining new information on the NP structure.

2. Materials and methods

2.1 Chemogenic and biogenic Selenium nanoparticle preparation

Chemogenic SeNPs were synthesized as described elsewhere (Piacenza et al., 2020a); Na_2SeO_3 (100 mM stock solution) was used at a final concentration of 0.5 mM, while L-cysteine concentration (50 mM stock solution) was varied to achieve 1:3 or 1:4 ratios to obtain a partial or total reduction of SeO_3^{2-}, respectively.
The bacterial strain *Micromonospora chockoriensis*, previously isolated from metal-rich Japanese wallpapers (Piacenza et al., 2020b), was chosen for SeNP synthesis. This strain was routinely pre-cultured in Luria Bertani (LB) rich medium for 72-h at 30°C with shaking (180 rpm) and subsequently inoculated (1% v/v) for 120-h at 30°C with shaking (180 rpm) in 250 mL Erlenmeyer flasks containing 50 mL of minimal medium (M9) amended with 0.5% (w/v) glucose and 0.5 mM Na_2SeO_3 as carbon and Se sources, respectively. The biogenic SeNP extracts were recovered following the procedure described by Piacenza et al. (2018c). To study the role of biomolecules within biogenic extracts in the thermodynamic stabilization of SeNPs, the latter were centrifuged (14000 *g* for 10 min) and the supernatant containing the organic material (OM) recovered, while biogenic SeNP pellet was resuspended in 1 ml of double distilled water (ddH_2O). L-cys SeNPs incubated with the OM were instead obtained as described by Piacenza and colleagues (2020a).
All the reagents were purchased from Sigma-Aldrich® (Milan, Italy). For clarity, the nomenclature and description of all the analysed samples are reported in Table 1.

Table 1: Nomenclature and description of the samples investigated

Samples	Description
L-cys SeNPs 1:3	SeNPs obtained using a 1-to-3 ratio between Na_2SeO_3 and L-cysteine
L-cys SeNPs 1:4	SeNPs obtained using a 1-to-4 ratio between Na_2SeO_3 and L-cysteine
Bio SeNP extract	Biogenic SeNP extract recovered from *M. chockoriensis* cells
Bio SeNP extract_w	Biogenic SeNP extract washed
OM	Organic material recovered from biogenic SeNP extract
L-cys SeNPs 1:4_OM	SeNPs obtained using a 1-to-4 ratio between Na_2SeO_3 and L-cysteine and incubated in the presence of the organic material

2.2 ATR-FTIR and ^{1}H-NMR spectroscopies

ATR-FTIR spectra were collected by using an FTIR Bruker Vertex70 Advanced Research FTIR Spectrometer (Billerica, MA, USA) equipped with a Platinum ATR and a diamond crystal. The spectra were recorded in the 40-4000 cm^{-1} range with a lateral resolution of 2 cm^{-1} and 200 scans.
The samples for ^{1}H NMR spectroscopy were prepared following the procedure in 2.1, substituting ddH_2O with D_2O (Cambridge Isotope Laboratories, Inc., MA, USA). ^{1}H NMR spectra were acquired through an FT-NMR Bruker Advance II 400 MHz with a pulse of 7.97 µs and 90°, and a delay time of 3 s. The HOD signal suppression was performed through a pulse field gradient (pulse sequence excitation sculpting) on the *z* axis. ATR-FTIR and ^{1}H NMR spectra were analysed through OPUS7.5, MestReNova, and OriginPro 2016 software.

2.3 Density Functional Theory (DFT) calculations

IR spectra of L-cysteine and its derivatives interacting with one Se_8 unit were simulated by calculating the harmonic vibrational frequencies and intensities within the DFT framework. The hybrid MO6-2X exchange - correlation function (Zhao et al., 2008) was chosen, whose reliability on treating systems where dispersion interactions are important is well-documented (Hoenstein et al., 2008). The correlation-consistent polarized double zeta (cc-pVDZ) was employed as basis set on all atoms. NMR shielding tensors were evaluated through the Gauge Including Atomic Orbitals approach, and chemical shifts are referred to TMS. Calculations were performed by using the Gaussian 16 program (Frisch et al., 2019).

3. Results and Discussion

Structural information regarding the samples listed in Table 1 was obtained through ATR-FTIR and NMR spectroscopies (Figures 1-2). Following the mechanism proposed by Painter (1941), a redox reaction occurring between thiol (SH)-containing molecules and Se(IV) (Na_2SeO_3) is responsible for the conversion of

the latter to Se(0) and the consequent oxidation of -SH groups. Se(IV) reduction was shown, in ATR-FTIR spectra, by either the disappearance (L-cys SeNPs 1:4) or the shift (L-cys SeNPs 1:3) towards longer wavenumber (ca. 2560 cm^{-1}) of the -SH stretching centred at ca. 2540 cm^{-1} typical of L-cysteine (Figure 1 a-b; Pawlukojc et al., 2005). The former implied that a complete reduction of Se(IV) was obtained for L-cys SeNPs 1:4 (Ganther 1971, Li et al., 2010), while the absorption band modification for L-cys SeNPs 1:3 was mostly caused by the presence of residual L-cysteine and its oxidation products. Indeed, defined and intense IR contributions in the 1630-250 cm^{-1} region, most of which appeared slighted shifted as compared to those observed for L-cysteine in solution, as well as vibrational mode attributable to the excess of Na_2SeO_3 (450-380 cm^{-1}; Figure 1 a-b; Makatun et al., 1970) were detected.

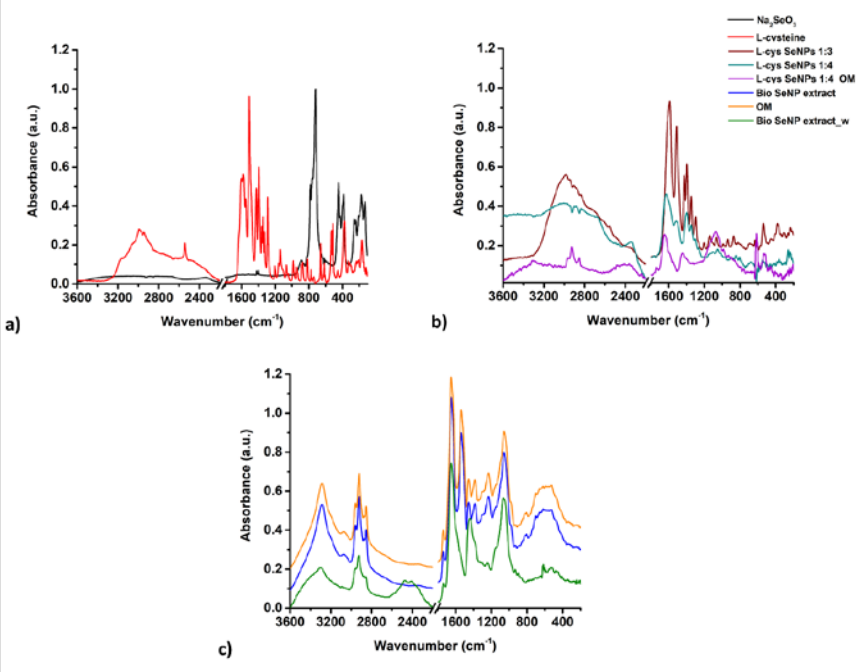

Figure 1: ATR-FTIR spectra of (a) L-cysteine and Na_2SeO_3, (b) chemogenic SeNPs, and (c) biogenic SeNP extracts and the recovered OM. For clarity, the spectra in (b-c) were offset by 0.1 a.u.

On the opposite, when the stoichiometric ratio (4:1) between L-cysteine and Na_2SeO_3 was used, no excess of Na_2SeO_3 was observed, L-cysteine was completely oxidised to cystine and derivatives (Li et al., 2010), and a large number of Se(0) atoms were available to generate SeNPs. Thus, since L-cysteine at the stoichiometric ratio acted as both reducing and surface modifier agent for SeNPs (Li et al., 2010), the derived oxidation products might more easily adsorb on SeNP surface, leading to the detection of few and broad IR absorption bands for L-cys SeNPs 1:4 (Figure 1 b), as highlighted by the similarity of these vibrational modes and those of chemical species simulated through DFT calculations (Tables S1-S2). ^{1}H-NMR spectroscopy underlined important differences both chemical shift and signal multiplicity for chemogenic SeNPs and L-cysteine (Figure 2 a). Lower chemical shift values were observed for $H_{\pm}$ of chemogenic SeNPs as compared to L-cysteine (ca. 3.88 ppm), which was more significant as the amount of amino acid increased (ca. 3.86 and 3.83 ppm for L-cys SeNPs 1:3 and 1:4, respectively), likely due to its oxidation and the simultaneous pH variation of the solutions (Ruks et al., 2019). In this regard, L-cysteine in ddH_2O featured a pH of ca. 4.5, while, upon its reaction with Se(IV), the solutions became more alkaline (*i.e.,* pH = 8 or 8.4 for L-cys SeNPs 1:3 and L-cys SeNPs 1:4, respectively). The importance of pH changes and L-cysteine oxidation in chemogenic SeNPs was highlighted by the detection of fewer vibrational modes attributable to the asymmetric or symmetric stretching of the protonated aminic group ($-NH_3^+$) in the 3100-2600 cm^{-1} region as compared to that of the amino acid (Figure 1 a-b), which was present in the zwitterionic form (Kurihara et al., 2019). NMR spectra also revealed a strong variation of chemical shift and coupling constant for H_{21} and H_{22} of L-cysteine when Na_2SeO_3 was added (Figure 2 a). Se(0) production resulted in a decreased electron density around the nuclei of H_{21} and H_{22}, as L-cysteine oxidation products were more electronegative compared to its -SH groups, leading to a deshielding of these protons. Since the chemical shift variation of H_{22} (ca. 0.2 ppm) was greater than for H_{21} (ca. 0.1 ppm) (Figure 2 b), the former appeared more influenced by the amino acid oxidation. Besides, an

overall change in H-multiplicity was observed for chemogenic SeNPs, as the H± signal became a quadruplet, while H²₁ and H²₂, although still multiplets, featured diverse contributions, which were more visible in the case of L-cys SeNPs 1:4 (Figure 2 a).

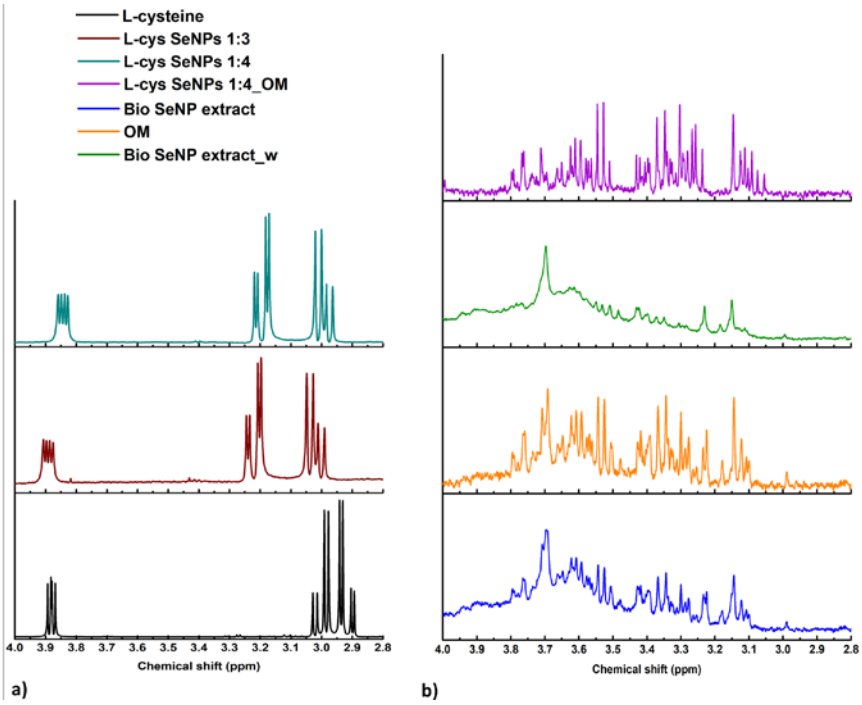

Figure 2: NMR spectra of (a) L-cysteine, (b) chemogenic SeNPs, and biogenic SeNP extracts and the recovered OM. For clarity, the spectra in (b) were offset by 1000 a.u.

On the other hand, ATR-FTIR and ^{1}H-NMR spectroscopies performed on Bio SeNP extract and the recovered OM showed a similar composition (Figures 1-2). In the case of NMR spectra, both Bio SeNP extract and OM featured several ^{1}H contributions (Figure 2 b) attributable to proteins, amino acid residues, glycolipids, aminoglycosides, and polysaccharides (Aspinall et al., 1994; Cox and Serpersu, 1995; Yeom et al., 2013; Morgan et al., 2020), even though no signal deriving from the ±-anomeric proton of the latter was observed at higher chemical shift values. Similar conclusions can be drawn by analysing the IR absorption bands observed in the 3300-2850 cm^{-1} region of these two samples (Figure 1 c), which were mostly ascribed to asymmetric and symmetric stretching of -NH, -NH_3^+, methyl (-CH_3), methylene (-CH_2) and methine (-CH) groups (Tugarova et al., 2018). More insights into the composition of biogenic samples were obtained through IR contributions in the 1750-250 cm^{-1} region, which revealed a strong absorbance of amine groups (1650-1250 cm^{-1}) typical of ±-helix (Amide II, ca. 1650 cm^{-1}) and ² -sheets (ca. 1630 cm^{-1}) proteins or free amino acids (Mohamed et al., 2013; Kamnev et al., 2017; Tugarova et al., 2018; Kristoffersen et al., 2020). Additionally, vibrational modes characteristic of (phospho)lipids, polysaccharides [±$_{(1,4)}$, ² $_{(1,4)}$, ±$_{(1,3)}$, ² $_{(1,3)}$ glycosidic bonds], nucleic acids, polyesters, and triglycerides were recognized (Nikonenko et al., 2000; Kamnev et al., 2017; Tugarova et al., 2018), implying the presence of multiple functional groups interacting with biogenic SeNPs. To better shed light on the structure of the biogenic extract and the roles of these biomolecules in the thermodynamic stabilization of SeNPs, Bio SeNP extract was washed to remove the excess of OM. The ^{1}H-NMR spectrum of BioSeNP extract_w showed fewer contributions compared to the unwashed one (Figure 2 b), being the majority typical of amino acids, proteins, aminoglycosides, and glycolipids (Aspinall et al., 1994; Cox and Serpersu, 1995; Yeom et al., 2013; Morgan et al., 2020), suggesting a preference of NH-containing biomolecules deriving from *M. chockoriensis* to be adsorbed on SeNP surface and to confer them a strong electrosteric stabilization (Piacenza et al., 2018b). Similarly, more intense and numerous IR signals deriving from functional groups such as -NH, -NH_3^+, alongside hydroxyl (-OH) and ammonium ion (-N^+H; 2490-2360 cm^{-1}) (Heacock and Marion, 1956), were detected in the washed sample as compared to Bio SeNP extract (Figure 1 c). Indeed, Bio SeNP extract_w featured NH-related IR bands similar to those observed for L-cysteine solution (Figure 1 a and c), implying that amino acid residues within the extract could be present in the zwitterionic form. Furthermore, vibrational modes characteristic of ±-helix and ² -sheets proteins, as well as

free amino acids, were detected in the 1650-1250 cm^{-1} region (Figure 1 c) of Bio SeNP extract_w, while the lower contribution of carboxylic moieties (Figure 1 c) can be due to the partial removal of COO^--containing molecules (*e.g.*, lipids and polysaccharides) by the washing procedure, which may indicate that these biomolecules were less prone to adsorb onto SeNP surface (Kamnev et al., 2017). Further support to this hypothesis was gained by analysing the ATR-FTIR and ^{1}H-NMR spectra of L-cys SeNPs 1:4 incubated with the OM recovered from *M. chockoriensis* cells (Figures 1 b and 2 b). Indeed, L-cys SeNPs 1:4_OM revealed strong IR absorption bands and ^{1}H signals belonging to L-cysteine oxidation products, (phospho)lipids, polyesters, nucleic acids, and polysaccharides (Nikonenko et al., 2000; Pawlukojc et al., 2005; Kamnev et al., 2017; Tugarova et al., 2018), while a lower number of contributions deriving from NH-containing molecules was observed (Figures 1 b and 2 b).

Besides the above-mentioned biomolecules, samples deriving from *M. chockoriensis* cells showed vibrational modes and ^{1}H contributions matching those obtained by DFT calculations for amino acid-like molecules containing -SH, sulfide ($-S^-$), sulfonyl ($-SO_2^-$), hydroxysulfoxyl ($-SO_2H$), sulfonate ($-SO_3^-$), and hydroxysulfonyl ($-SO_3H$) groups adsorbed on the SeNP surface (Tables S1-S2), being these signals more prominent in the case of the Bio SeNP extract_w. This evidence, alongside the detection in ^{1}H-NMR spectra of biogenic extracts and the recovered OM of chemical shift likely attributable to glutathione disulphide (GSSG; Millis et al., 1993), supports the involvement of sulphur- and thiol-containing molecules (*e.g.,* mycothiols) in the biotransformation of selenite oxyanions by *M. chockoriensis* strain, as well as their partial contribution to the stabilization of biogenic SeNPs (Presentato et al., 2018).

4. Conclusions

The structural characterization of eco- and bio-compatible SeNPs highlighted differences and similarities between chemogenic and biogenic synthetic procedures. In both cases, sulphur- and thiol-containing molecules appear to mediate the reduction of Se(IV) to Se(0), yet biogenic SeNP extracts were more complex. A common trait between chemogenic and biogenic samples was the presence of NH-containing molecules (*e.g.,* free amino acids or derivatives, ±-helix, and ²-sheets proteins) preferentially adsorbing onto SeNP surface and contributing to their thermodynamic stabilization. In this regard, although other biomolecules detected in the biogenic extract or its derived OM were partially removed by a washing step, SeNPs remained stable in solution, indicating the occurrence of strong electrosteric interactions between NH-containing biomolecules adsorbed on the surface of NPs and the NPs themselves.

Acknowledgments

We greatly acknowledge the L'Oréal – UNESCO "For Women In Science" award (Italian edition 2020) for funding EP's research, the National Interuniversity Consortium of Materials Science and Technology (EP and DFCM), and Dr. Alberto Spinella [Advanced Technologies Network (ATeN) Center, Palermo] for performing ^{1}H NMR spectroscopy.

References

Rao C.N.R., Muller A., Cheetham A.K., 2004, The Chemistry of Nanomaterials: Synthesis, Properties and Applications. WILEY-VCH Verlag GmbH & Co. KgaA, Weinheim, Germany, 1 – 11.

Piacenza E., Presentato A., Zonaro E., Lampis S., Vallini G., Turner R.J. 2018a, Selenium and Tellurium Nanomaterials. Physical Sciences Reviews, 3, 20170100.

Khurana A., Tekula S., Saifi M.A., Venkatesh P., Godugu C., 2019, Therapeutic applications of selenium nanoparticles, Biomedicine & Pharmacotherapy,111, 802 – 812.

Shoeibi S., Mozdziak P., Golkar-Narenji A., 2017, Biogenesis of Selenium Nanoparticles Using Green Chemistry. Topics in Current Chemistry, 375, 88.

Piacenza E., Presentato A., Turner R.J., 2018b, Stability of biogenic metal(loid) nanomaterials related to the colloidal stabilization theory of chemical nanostructures, Critical Review in Biotechnology, 38, 1137 – 1156.

Li Q., Chen T., Yang F., Liu J., Zheng W., 2010, Facile and controllable one-step fabrication of selenium nanoparticles assisted by L-cysteine. Material Letters, 64, 614 – 617.

Piacenza E., Presentato A., Heyne B., Turner R.J., Tunable photoluminescence properties of Selenium nanoparticles: biogenic *vs* chemogenic synthesis, Nanophotonics, 2020a, 9, 3615 – 3628.

Piacenza E., Presentato A., Di Salvo F., Alduina R., Ferrara V., Minore V., Giannusa A., Sancataldo G., Chillura Martino D.F., 2020b, A combined physical-chemical and microbiological approach to unveil the fabrication, provenance, and state of conservation of the *Kinkarakawa-gami* art, Scientific Reports, 10, 16072.

Piacenza E, Presentato A, Ambrosi E, Speghini A., Turner R.J., Vallini G., Lampis S., 2018c, Physical-chemical properties of biogenic selenium nanostructures produced by *Stenotrophomonas maltophilia* SeITE02 and *Ochrobactrum* sp. MPV1 strains, Frontiers in Microbiology, 9, 3178.

Painter E.P., The chemistry and toxicity of Selenium compounds, with special reference to the Selenium problem, 1941, Chemical Reviews, 28, 179 – 213.

Ganther H.E., 1971, Reduction of the selenotrisulfide derivative of glutathione to a persulfide analog by glutathione reductase, Biochemistry, 10, 4089 – 4098.

Pawlukojc A., Leciejewicz J., Ramirez-Cuesta A.J., Nowicka-Scheibe J., 2005, L-cysteine: neutron spectroscopy, Raman, IR and ab initio study, Spectrochimica acta. Part a, Molecular and Biomolecular Spectroscopy, 61, 2474 – 2481.

Makatun V.N., Pechkovskii V.V., Mel'nikova R.Y., Gusev S.S., 1970, Infrared spectra of copper selenites, Zhurnal Prikladnoi Spektroskopii, 12, 497 – 503.

Kurihara T., Noda Y., Takegoshi K., 2019, Capping structure of ligand-cysteine on CdSe magic-sized clusters, ACS Omega, 4, 3476 – 3483.

Ruks T., Beuck C., Schaller T., Niemeyer F., Zahres M., Loza K., Heggen M., Hagemann U., Mayer C., Bayer P., Epple M., 2019, Solution NMR spectroscopy with isotope-labeled cysteine (^{13}C and ^{15}N) reveals the surface structure of L-cysteine-coated ultrasmall gold nanoparticles (1.8 nm), Langmuir, 35, 767 – 768.

Aspinall G.O., McDonald A.G., Pang H., Kurjanczyk L.A., Penner J.L., 1994, Lipopolysaccharides of *Campylobacter jejuni* serotype):19: structures of core oligosaccharide regions from the serostrain and two bacterial isolates from patients with the Guillain-Barré syndrome, Biochemistry, 33, 241 – 249.

Cox J.R., Serpersu E.H., 1995, The complete ^{1}H NMR assignements of aminoglycoside antibiotics and conformational studies of butirosin A through the use of 2D NMR spectroscopy, Carbohydrate Research, 271, 55 – 63.

Yeom J., Shin J.H., Yang J.Y., Kim J., Hwang G.S., 2013, ^{1}H NMR-based metabolite profiling of planktonic and biofilm cells in *Acinetobacter baumannii* 1656-2, PLOS ONE, 8, e57730.

Morgan K.T., Zheng J., McCafferty D.G., 2020, Targeted Genome mining discovery of the ramoplanin congener chersinamycin from the dynemicin-producer *Micromonospora chersina* DSM 44154, bioRxiv 2020.05.22.111625; doi: 10.1101/2020.05.22.111625

Tugarova A.V., Mamchenkova P.V., Dyatlova Y.A., Kamnev A.A., 2018, FTIR and Raman spectroscopic studies of selenium nanoparticles synthesized by the bacterium *Azospirillum thiophilum*, Spectrochimica Acta Part A: Molecular and Biomolecular Spectroscopy, 192, 458 – 463.

Mohamed M.E., Mohammed A.M.A., 2013, Experimental and computational vibration study of amino acids, International Letters of Chemistry, Physics and Astronomy, 10, 1 – 17.

Kamnev A.A., Mamchenkova P.V., Dyatlova Y.A., Tugarova A.V., 2017, FTIR spectroscopic studies of selenite reduction by cells of the rhizobacterium *Azospirillum brasilense* Sp7 and the formation of selenium nanoparticles, Journal of Molecular Structure, 1140, 106 – 112.

Kristoffersen K.A., van Amerongen A., Bocker U., Lindberg D., Wubshet S.G., de Hogel-van den Bosch H., Horn S.J., Afseth N.K., 2020, Fourier-tranform infrared spectroscopy for monitoring proteolytic reactions using dry-films treated with trifluoroacetic acid, Scientific Reports, 10, 7844.

Nikonenko N.A., Buslov D.K., Sushko N.I., Zhbankov R.G., 2000, Investigation of stretching vibrations of glycosidic linkages in disaccharides and polysaccharides with use of IR spectra deconvolution, Biopolymers, 57, 257 – 262.

Heacock R.A., Marion L., 1956, The Infrared spectra of secondary amines and their salts, Canadian Journal of Chemistry, 34, 12.

Millis K.K., Weaver K.H., Rabenstein D.L., 1993, Oxidation/reduction potential of glutathione, Journal of Organic Chemistry, 58, 4144 – 4146.

Presentato A., Piacenza E., Anikovkiy M., Cappelletti M., Zannoni D., Turner R.J., 2018, Biosynthesis of selenium nanoparticles and nanorods as a product of selenite bioconversion by the aerobic bacterium *Rhodococcus aetherivorans* BCP1, New Biotechnology, 41, 1 – 8.

Zhao Y., Truhlar D.G., 2008, The M06 suite of density functionals for main group thermochemistry, thermochemical kinetics, noncovalent interactions, excited states, and transition elements: two new functionals and systematic testing of four M06-class functionals and 12 other functionals, Theoretical Chemistry Account, 120, 215 – 241.

Hohenstein E.G., Chill S.T., Sherrill C.D., 2008, Assesment of the performance of the M05-2X ad M06-2X exchange-correlation functionals for noncovalent interactions in biomolecules. Journal of Chemical Theory and Computation, 4, 1996 – 2000.

Frisch M.J., 2019, Gaussian 16, Revision C.01, Gaussian, Inc., Wallingford CT, https://gaussian.com/citation/